Effects of the Gaseous and Liquid Water Content of the Atmosphere on Range Delay and Doppler Frequency

W. L. Flock
Telecommunications Systems Section

When high precision is required for range measurement on Earth-space paths, it is necessary to correct as accurately as possible for excess range delays due to the dry air, water vapor, and liquid water content of the atmosphere. Calculations based on representative values of atmospheric parameters are useful for illustrating the order of magnitude of the expected delays. Range delay, time delay, and phase delay are simply and directly related. Doppler frequency variations or noise are proportional to the time rate of change of excess range delay.

I. Introduction

Increasingly sophisticated deep-space missions place high requirements upon the precision of time delay and Doppler frequency measurements. The interplanetary plasma is one of the factors limiting the precision of such measurements. The excess time and range delays due to the plasma are proportional to total electron content along the path and inversely proportional to frequency squared. Doppler frequency variations are generated by the plasma in direct proportion to the rate of change of total electron content and in inverse relation with frequency. When unwanted, as is often the case, such variations are commonly referred to as Doppler frequency noise. In deep-space missions conducted by the Jet Propulsion Laboratory, range has been determined by using coded two-way transmissions at S-band for the uplink and S-band and X-band for the downlink. Because of the need for increased precision in range and Doppler frequency measurement, it is planned to demonstrate the capability of the higher frequency X-band for both the uplink and downlink, retaining S-band up- and downlinks as well. K-band links may be utilized at a later date. High precision is needed for range measurements when using very long baseline interferometry (VLBI) techniques, and high precision and sensitivity for Doppler frequency measurements are required if gravitational waves are to be recorded (Refs. 1 and 2).

When high precision is needed for range and Doppler frequency measurements, it becomes necessary to consider effects due to the gaseous and liquid water content of the troposphere as well as effects due to the interplanetary plasma and ionosphere. The tropospheric effects may dominate if the interplanetary plasma Doppler noise is reduced by adding X-band uplink capability (Ref. 3). The purpose of this report is to analyze the tropospheric effects as part of an overall consideration of the capability of precision two-way ranging and Doppler systems.

The term precision is used here in distinction from accuracy. The state of knowledge concerning the velocity of light limits the absolute accuracy of range measurements, but it is possible to overcome propagation effects and hardware limitations sufficiently to obtain high precision and a high degree of consistency.

II. Excess Range Delay Due to Dry Air and Water Vapor

A. Refractivity of Troposphere

Range to a target is commonly determined by radar techniques by assuming that electromagnetic waves propagate with the velocity c (2.99792458×10^8 m/s or approximately 3×10^8 m/s). A velocity of c corresponds to an index of refraction of unity. In the troposphere, however, the index of refraction n is slightly greater than unity with the result that the phase velocity of an electromagnetic wave is slightly less than c. A range error then results if the velocity c is assumed. The slight error in range is unimportant in many applications, but may be important in other situations. In practice, when high precision in range is desired, it is anticipated that the range indicated by using the velocity c is greater than the true range, and an effort is made to estimate as closely as possible the excess range delay ΔR (the amount by which the indicated range exceeds the true range) in order to correct for it.

To consider the excess range delay, which can be referred to also as excess group delay, note that the integral $\int n\,dl$ evaluated along a path, with n representing the index of refraction and dl an increment of length, gives the true distance along the path if $n = 1$, but gives a value which is different from the true distance if $n \neq 1$. (By definition, the index of refraction n of a particular wave type in a given medium is the ratio of c to v_p, the phase velocity of the wave in the medium.) The difference ΔR between the true and indicated distances is given by

$$\Delta R = \int (n - 1)\,dl \tag{1}$$

The index of refraction of the troposphere is only slightly greater than 1 and for this reason the usual practice is to use N units, defined by $N = (n - 1)10^6$ and commonly referred to as refractivity. The refractivity of the troposphere is given by

$$N = \frac{77.6\,p_d}{T} + \frac{72\,e}{T} + \frac{3.75 \times 10^5\,e}{T^2} \tag{2}$$

where p_d is the pressure of dry nonpolar air in millibars (mb), e is water vapor pressure in mb, and T is absolute temperature in kelvins (Ref. 4). N is seen to vary inversely with temperature and to be strongly dependent on water vapor pressure e, which equals the saturation water vapor pressure e_s times the relative humidity, RH. The saturation water vapor pressure e_s is a function of temperature as shown in Table 1.

If Equation (2) is expressed in terms of total pressure p, where $p = p_d + e$, it becomes

$$N = \frac{77.6\,p}{T} - \frac{5.6\,e}{T} + \frac{3.75 \times 10^5\,e}{T^2} \tag{3}$$

The last two terms can be combined to give, approximately,

$$N = \frac{77.6\,p}{T} + \frac{3.73 \times 10^5\,e}{T^2} \tag{4}$$

The form is widely used and gives values for N that are accurate within 0.5 percent for the ranges of atmospheric parameters normally encountered and for frequencies below 30 GHz (Ref. 6). If one wishes to consider separately the effects of dry air and water vapor, however, with $N = N_d + N_w$ where N_d refers to dry air and N_w to water vapor, Eq. (2) should be used with

$$N_d = \frac{77.6\,p_d}{T} \tag{5}$$

and

$$N_w = \frac{72\,e}{T} + \frac{3.75 \times 10^5\,e}{T^2} \tag{6}$$

B. Excess Range Delay Due to Dry Air

We consider first the magnitude of ΔR_d, the excess range due to dry air, for a zenith path. For this purpose, SI units will be used with p_d in newtons/meter^2 (N/m^2) rather than mb. Then $N_d = 0.776\,p_d/T$ and, by using Eq. (A-3) of the Appendix, p_d/T is replaced by $R\rho/M$ so that

$$N_d = \frac{0.776\,R\rho}{M} \tag{7}$$

where R is the gas constant, 8.3143×10^3 J/(K kg mol) with J standing for joules. M is the molecular weight in kg mol and is taken as 28.8 corresponding to an atmosphere that is 80 percent molecular nitrogen and 20 percent molecular oxygen. The density ρ in Eq. (7) is in kg/m^3. ΔR_d, the excess range delay due to dry air, can be calculated for a zenith path in terms of N_d by

$$\Delta R_d = 10^{-6} \int N_d \, dh = \frac{10^{-6}\, 0.776\, R}{M} \int_0^{\infty} \rho \, dh \qquad (8)$$

The surface pressure p_0 is related to density ρ by

$$p_0 = g \int \rho \, dh \qquad (9)$$

where g is the acceleration of gravity and has the value of 9.8 m/s^2 at the Earth's surface. The resulting approximate expression for ΔR_d, using this surface value of g, is

$$\Delta R_d = \frac{(0.776)\,(8.3143 \times 10^3)}{(28.8)\,(9.8)\,(10^6)} p_0$$

so that

$$\Delta R_d = 2.29 \times 10^{-5}\, p_0, \mathrm{m} \qquad (10a)$$

with p_0 in N/m^2 and

$$\Delta R_d = 2.29 \times 10^{-3}\, p_0, \mathrm{m} \qquad (10b)$$

with p_0 in mb. The pressure p_0 is the surface pressure of dry air and equals total pressure p minus water vapor pressure e. Note that the temperature T drops out and the result depends on surface pressure p_0 only. If $p_0 = 1000$ mb, $\Delta R_d = 2.29$ m. Hopfield (Ref. 7) has examined the applicability of this relation and, using 2.2757 as the coefficient corresponding to the value of g at about 6 km above sea level, has concluded that it allows determination of the range error due to dry air on a zenith path to an accuracy of 0.2 percent or about 0.5 cm. Her form for Eq. (10) is

$$\Delta R_d = 2.2757 \times 10^{-3}\, p_0 \qquad (10c)$$

with p_0 in mb.

C. Excess Range Delay Due to Water Vapor

The delay caused by water vapor is considerably smaller than that for dry air, but total water vapor content along a path is variable and not predictable with high accuracy from the surface water vapor pressure. Therefore, water vapor is responsible for a larger error on uncertainty in range than dry air. N_w can be expressed in terms of water vapor density ρ rather than water vapor pressure e by using

$$e = \frac{\rho T}{216.7} \qquad (11)$$

as derived in the Appendix, with ρ in g/m^3 and e in mb. N_w then takes the form

$$N_w = 0.3323\, \rho + \frac{1.731 \times 10^3\, \rho}{T} \qquad (12)$$

from which

$$\Delta R_w = 10^{-6} \int N_w \, dl = 3.323 \times 10^{-7} \int \rho \, dl + 1.731 \times 10^{-3} \int \frac{\rho}{T} dl, \mathrm{m} \qquad (13)$$

Sometimes the first term of Eqs. (12) and (13) is not used, but for highest accuracy it should be retained. For example, if 1.731×10^3 is divided by a temperature near 280 K, then the first term amounts to about 5 percent of the total delay. The value of the integral of Eq. (13) can be determined from radiosonde data, assuming that ρ and T vary only with height above the surface and not horizontally to a significant degree within the limits of the path.

Microwave radiometry has the advantage of being able to provide continuous real-time estimation of ΔR_w by use of remote sensing techniques. The basic relation utilized for microwave radiometry applies to the brightness temperature T_b that is observed, when a source at a temperature of T_s is viewed through an absorbing medium having a variable temperature T. T_b is given by (Ref. 8)

$$T_b = T_s e^{-\tau_\infty} + \int_0^{\infty} T(h)\, \alpha(h)\, e^{-\tau}\, dh \qquad (14)$$

with

$$\tau_\infty = \int_0^\infty \alpha(h)\, dh$$

and

$$\tau = \int_0^h \alpha(h)\, dh$$

where $\alpha(h)$ is the attenuation constant that is a function of height h. The expression for T_b takes a simpler form when T is constant or when an effective value T_i can be employed. In that case

$$T_b = T_s e^{-\tau} + T_i (1 - e^{-\tau}) \tag{15}$$

which form is used for remote sensing of attenuation due to precipitation. The source temperature T_s represents cosmic noise in the case considered here and has a small value. Therefore, attention is directed primarily to the second term of Eq. (14). The attenuation constant $\alpha(h)$ is due to three forms of matter: water vapor, the liquid water of clouds, and oxygen. To obtain information on water vapor, for example, it is necessary to separate out the effects of liquid water and oxygen. The separation can be accomplished by making observations at 2 or more frequencies.

Consider first the problem of obtaining the total water vapor and liquid water content along a tropospheric zenith path. For this purpose, one can use a pair of frequencies such as 20.6 GHz and 31.6 GHz, the first near the peak of and thus sensitive to water vapor absorption and the second more sensitive to liquid water than to water vapor. Taking this approach, M_V and M_L, the total vapor and liquid contents in g/cm^2, can be obtained from (Refs. 9 and 10)

$$M_V = a_1 + a_2 T_{b_2} + a_3 T_{b_3} \tag{16}$$

and

$$M_L = b_1 + b_2 T_{b_2} + b_3 T_{b_3} \tag{17}$$

where T_{b_2} is the brightness temperature at the lower frequency and T_{b_3} is the brightness temperature at the higher frequency. The a's and b's are determined by a process of statistical inversion. Simultaneous radiosonde data and readings of brightness temperature are utilized to carry out this process. For Denver, Colorado, the particular relation obtained is

$$M_V = -0.18 + 0.11\, T_{b_2} - 0.053\, T_{b_3}$$

$$M_L = -0.017 - 0.001\, T_{b_2} + 0.0027\, T_{b_3}$$

The relative sensitivities to water vapor and liquid water are shown by the relative magnitudes of a_2 and a_3 for water vapor and b_2 and b_3 for liquid water. The coefficients a_1 and b_1 take account of oxygen and cosmic noise.

For range delay due to water vapor, however, the integral $\int \rho/T\, dh$ makes a larger contribution than $\int \rho\, dh = M_V$. For determining $\int \rho/T\, dh$, using two frequencies similar to those mentioned above, and therefore, utilizing two equations having the form of Eq. (14), leads to (Ref. 11)

$$\frac{T_{b_1} - T_{c_1}}{f_1^2} - \frac{T_{b_2} - T_{c_2}}{f_2^2} = \int_0^\infty W(h) \frac{\rho}{T}\, dh + T_0 \tag{18}$$

where

$$W(h) = \frac{T^2}{\rho} \left[\frac{\alpha_{v_1}}{f_1^2} e^{-\tau_1} - \frac{\alpha_{v_2}}{f_2^2} e^{-\tau_2} \right] \tag{19}$$

and

$$T_0 = \int_0^\infty T \left[\frac{\alpha_{0_1} e^{-\tau_1}}{f_1^2} - \frac{\alpha_{0_2} e^{-\tau_2}}{f_2^2} \right] \tag{20}$$

The total attenuation α is the sum of three contributions so that

$$\alpha = \alpha_V + \alpha_L + \alpha_O \tag{21}$$

where α_V is the attenuation constant associated with water vapor, α_L is that associated with liquid water, and α_O is associated with oxygen. By assuming that α_L for clouds varies as f_1^2, α_L has been eliminated and the factors of f_1^2 and f_2^2 appear in the denominators as shown. T_{c_1} and T_{c_2} represent values of the first term of Eq. (14) and, being small, are treated as constants. By suitable choice of frequencies and other refinements, $W(h)$ is made to assume an essentially constant known value so that $\int_0^\infty \rho/T\, dh$ can be determined. Pairs of frequencies that have been found to be satisfactory are

20.3 and 31.4 GHz, 20.0 and 26.5 GHz, and 24.5 and 31.4 GHz (Ref. 11).

The development and testing of water vapor radiometers has received considerable attention at the Jet Propulsion Laboratory (Refs. 11 through 15). One of the systems developed utilized 18.5 and 22.235 GHz as the frequency pair, this combination having the advantage of using the same size of waveguide for both frequencies (Ref. 14). It was concluded later, however, that the 20.3 and 31.4 GHz pair provided better performance.

Profiles of tropospheric temperature can also be obtained by microwave radiometry utilizing three frequencies near the 60-GHz oxygen absorption peak and one frequency each near 20 GHz and 30 GHz to separate out water vapor and liquid water effects (Ref. 10). Oxygen is a major constituent of and occurs as an essentially fixed fraction of the tropospheric composition, and the temperature of oxygen at a given height is thus the temperature of the troposphere at that height. The frequencies utilized allow a coarse determination of the water vapor profile as well, but the use of several frequencies near the peak of a strong water vapor absorption line such as that at 183 GHz is stated to be necessary to provide accurate profiles of water vapor content (Ref. 10).

D. Illustrative Calculated and Measured Values of Excess Delay Due to Water Vapor

The precise value of ΔR_w in a particular situation depends on the water vapor and temperature profiles, but an indication of the magnitude of ΔR_w can be obtained by assuming an exponential decrease of N_w with a scale height H of 2 km, a water vapor density ρ at the surface of 7.5 g/m^3, and a temperature of 281.65 K (that for a standard atmosphere at an altitude of 1 km). It is of interest that the value obtained for ΔR_w in this way is the same as if N_w were constant up to the height H and zero beyond. The values of 7.5 g/m^3 and 2 km are mentioned as being representative values in CCIR Report 719 (Ref. 16). The values of ρ and T at the surface result in values of e and N_w of 9.748 mb and 48.57, respectively. Then, for a zenith path,

$$\Delta R_w = 10^{-6} \int_0^\infty 48.57\, e^{-h/2000}\, dh$$

$$= 10^{-6}\,(48.57)\,(2000) = 0.0972 \text{ m}$$

$$= 9.72 \text{ cm} \tag{22}$$

The excess range due to water vapor for a zenith path may thus be about 10 cm. For paths at elevation angle θ of about 10 deg or greater, the range delay equals the zenith value divided by sin θ. That is,

$$\Delta R(\theta) = \frac{\Delta R\,(\theta = 90 \text{ deg})}{\sin\theta} \tag{23}$$

For an elevation angle of 30 deg, for example, ΔR_w might be about 20 cm.

An extreme value of 44.8 cm for ΔR_w for a zenith path could occur for the highest accepted weather observatory values for e and ρ of 53.2 mb and 37.6 g/m^3, respectively, at the temperature of 34°C (Ref. 17). These values were recorded at Sharjah, Saudi Arabia, on the Persian Gulf. The value of ΔR_w of 44.8 cm is based on an exponential decrease of N_w with a scale height of 2 km as in the previous example.

Mean zenith values of ΔR_w determined from radiosonde measurements in a semiarid location in California ranged from 4 to 16 cm (Ref. 18). With respect to the accuracy to which ΔR_w can be determined, Wu (Ref. 11) stated that the calibration for water vapor delay, using a water vapor radiometer, is accurate to <2 cm at all elevation angles greater than 15 deg. Slobin and Batelaan (Ref. 15) state that the rms error in ΔR_w, as determined by a water vapor radiometer, was less than 1 cm over a total delay range of 9 to 38 cm at a 30 deg elevation angle.

E. Time Delay

Range delay and time delay are directly related. If one prefers to think in terms of time delay Δt or wishes to determine numerical values of time delay corresponding to values of range delay, use

$$\Delta t = \frac{\Delta R}{c} \tag{24}$$

for one-way paths. For monostatic radar modes of operation for which electromagnetic waves twice traverse the distance from the original transmitter to the target or repeater,

$$\Delta t = \frac{2\Delta R}{c} \tag{25}$$

A range delay of 10 cm for water vapor on a one-way path corresponds to a time delay of 0.333 ns. The extreme range delay on a one-way zenith path of 44.8 cm is equivalent to a time delay of 1.5 ns.

III. Excess Range Delay Due to Liquid Water

A. Effective Index of Refraction of Medium

The liquid water content of the troposphere can also make a contribution to range delay. To distinguish the range delays due to water vapor and liquid water, we shall henceforth use ΔR_1 for the delay due to water vapor and ΔR_2 for the contribution due to liquid water. To determine ΔR_2 due to the small droplets of clouds, one can make use of the fact that a small spherical particle in the presence of a sinusoidally time-varying electric field acts as a tiny antenna having an electric dipole moment p_1. By application of Laplace's equation (Ref. 19, pp. 218 to 224, for example), it can be shown that, when the drop diameter is small compared to wavelength, p_1 is given by

$$p_1 = 3V\left(\frac{n^2 - 1}{n^2 + 2}\right)\epsilon_0 E_0 \tag{26}$$

where V is the volume of the spherical particle and n is now the index of refraction of the particle, in the case of interest here the index of refraction of water. The quantity ϵ_0 is the electric permittivity of empty space (8.854×10^{-12} F/m) and E_0 is the electric field intensity of the incident wave in V/m. In a region containing N such particles per unit volume

$$P = Np_1 = 3NV\left(\frac{n^2 - 1}{n^2 + 2}\right)\epsilon_0 E_0 \tag{27}$$

where P is the electric dipole moment or electric polarization per unit volume (considering only the effect of the spherical water particles and neglecting all other possible contributions to P). The basic relations, by definition, between E, D (electric flux density), and P for an isotropic medium are that

$$D = \epsilon_0 E + P = \epsilon_0 (1 + \chi)E = \epsilon_0 KE \tag{28}$$

where K is the relative dielectric constant and χ is electric susceptibility. The relative dielectric constant K (commonly designated by ϵ_r) is equal to ϵ/ϵ_0, where ϵ is the electric permittivity of the medium. D and P have units of C/m^2. From Eq. (28),

$$K = 1 + \chi \tag{29}$$

In the case considered here, K is an effective relative dielectric constant of a medium consisting of small spherical water droplets in empty space.

The excess range delay in the medium is proportional to the index of refraction of the medium minus unity as in Eq. (1). As n has already been used in Section III for the index of refraction of water, however, we will use m for the index of refraction of the medium. Index of refraction squared equals relative dielectric constant. Thus

$$m^2 = K \tag{30}$$

Then as, in general, $(1 + a)^{1/2} = 1 + a/2$ for $a \ll 1$ and in this case χ is much less than 1,

$$m = 1 + \frac{\chi}{2} \tag{31}$$

By comparison of Eqs. (27) and (28),

$$\chi = 3NV\left(\frac{n^2 - 1}{n^2 + 2}\right) \tag{32}$$

and

$$m - 1 = \frac{\chi}{2} = \frac{3NV}{2}\left(\frac{n^2 - 1}{n^2 + 2}\right) \tag{33}$$

The relation comparable to Eq. (1) for determining the excess range delay ΔR_2 due to the liquid water content of the troposphere is

$$\Delta R_2 = \int Re\,(m - 1)\,dl \tag{34}$$

Here m is used in place of the n of Eq. (1) and the expression indicates that the real part of $m - 1$ should be used. This notation is needed because the index of refraction of water is complex and m is therefore complex also. The real part of m determines the phase shift and range delay, and the imaginary part determines attenuation. In deriving Eq. (33), no mention was made of the lossy nature of the droplets, but relations derived for a lossless medium can be applied to the lossy case by merely utilizing the proper complex value in place of the real value. Whereas the index of refraction of dry air and water vapor are independent of frequency in the radio frequency range up to about 50 GHz, the index of refraction of liquid water is a function of frequency and temperature.

B. Illustration of Excess Range Delay Due to a Cloud

To illustrate the range delay due to water droplets in a cloud, consider the range delay for a zenith path through a dense cloud 1-km thick and having a water content of 1 g/m^3. For a frequency of $f = 3$ GHz and a temperature of $T = 20$°C, it can be determined from curves given by Zufferey (Ref. 20) (see also Hogg and Chu (Ref. 21), or values presented by Gunn and East (Ref. 22)), that $n = 8.88 - j\,0.63$. As water has a density of 1 g/cm^3, the water content of 1 g/m^3 fills only 10^{-6} of a cubic meter. Then NV of Eq. (33) is 10^{-6} so that

$$m - 1 = \frac{3}{2}10^{-6}\left[\frac{(8.88 - j\,0.63)^2 - 1}{(8.88 - j\,0.63)^2 + 2}\right]$$

and

$$Re\,(m - 1) = 3/2\,(0.967)\,(10^{-6})$$

$$= 1.45 \times 10^{-6}$$

As a region of uniform water content and a thickness of 1 km is assumed, the integral of Eq. (26) simplifies to become the product of $Re\,(m - 1)$ and 10^3 m so that

$$R_2 = 1.45 \times 10^{-6}\,(10^3)$$

$$= 1.45 \times 10^{-3}\ \text{m}$$

$$= 0.145\ \text{cm}$$

For $f = 10$ GHz, $n = 8.2 - j\,1.8$ and the value of ΔR_2 is 0.144 cm, while for $f = 30$ GHz, $n = 6 - j\,2.8$ but ΔR_2 is still about 0.144 cm. The excess range delay in this case is quite insensitive to the value of n, which condition might be anticipated by noting that n^2 appears in both the numerator and denominator of Eq. (33). The excess delay is therefore insensitive to frequency as well.

The water content of 1 g/m^3 assumed in the above example is that of a rather dense cloud, but it has been reported that the maximum water content of clouds lies between 6 and 10 g/m^3 (Ref. 23).

C. Excess Range Delay Due to Rain

Raindrops are considerably larger than the small droplets of clouds, and to analyze the effects of raindrops one must generally use the Mie scattering theory or refinements of it. The technique of deriving an equivalent index of refraction can nevertheless be employed for rain; this approach has been utilized most extensively for determining the attenuation constant for propagation through rain. If $m = m_r - jm_i$, the field intensity attenuation constant α is given by

$$\alpha = \beta_0\, m_i \ \text{neper/m} \qquad (35)$$

where $\beta_0 = 2\pi/\lambda_0$ is the phase constant and λ_0 is wavelength for propagation in empty space. (One neper equals 8.68 dB.) The phase constant β for propagation through a region of rain is given by

$$\beta = \beta_0\, m_r \ \text{rad/m} \qquad (36)$$

For calculating the excess range delay ΔR_2 due to rain, one can use

$$\int Re\,(m - 1)\,dl = \int (m_r - 1)\,dl \qquad (37)$$

Tables giving values of $m_r - 1$ have been provided by Setzer (Ref. 24), and Zufferey (Ref. 20) has presented these values in graphical form (Fig. 1). Setzer's value for $m_r - 1$ for a rain of 25 mm/h at a frequency of 3 GHz, for example, is 1.8×10^{-6}. The excess range delay in a 1-km path of uniform rain of that rate is $(1.8 \times 10^{-6})\,(10^3) = 0.18$ cm, a value comparable to that for a zenith path through a cloud 1-km thick. For a heavy rain of 150 mm/h, the delay would be 0.92 cm in 1 km.

For estimating total excess range delay due to rain, one needs an estimate of effective path length through rain. This topic of effective path length has been considered with respect to estimating attenuation due to rain (Refs. 25, 26). Rain is largely confined below the 0°C isotherm, and the height of the isotherm and the elevation angle of the path determine the path length through rain. In addition, it develops that the average rain rate along a path tends to differ from the instantaneous point rain rate, the average rate being less than the point rate for heavy rains. Effective path lengths through rain tend to be in the order of 4 or 5 km for an elevation angle of 45 deg at a latitude of 40°N (Ref. 20) and these figures can be used as a rough guide. Information on the height of the 0°C isotherm as a function of probability of occurrence is given in Fig. 2. In contrast with attenuation in rain which increases with frequency up to about 150 GHz, excess range delay decreases above 10 GHz and stays nearly constant below 10 GHz to 1 GHz or lower, but has modest maxima in the 6- to 10-Ghz range, depending on rain rate (Fig. 1). It appears that the excess range delay due to rain may be of significance in some heavy rainstorms.

The concept of an equivalent index of refraction of a medium containing small particles has been discussed by van de Hulst (Ref. 27) and Kerker (Ref. 28), but early consideration of this topic is attributed by Kerker to an 1899 paper by Rayleigh and 1890 and 1898 papers by Lorenz.

IV. Phase Delay and Doppler Frequency

A. Relations Between Range and Time Delay, Phase Delay, and Doppler Frequency

Range delay, time delay, and phase delay are all directly and simply related. It was pointed out in Section II that time delay Δt is related to range delay ΔR by

$$\Delta t = \frac{\Delta R}{c}$$

for a one-way path. The phase delay $\Delta\phi$ associated with a range delay can be determined by taking the product of the range delay ΔR and the phase constant β_0. Thus

$$\Delta\phi = \beta_0 \Delta R = \frac{2\pi}{\lambda_0}\Delta R = \frac{2\pi f}{c}\Delta R \qquad (38)$$

Doppler frequency f_D and phase ϕ are related by

$$f_D = \frac{1}{2\pi}\frac{d\phi}{dt}, \text{Hz} \qquad (39)$$

This relation can also be written in terms of finite quantities as

$$f_D = \frac{1}{2\pi}\frac{\Delta\phi}{T_c}, \text{Hz} \qquad (40)$$

where T_c is a count time or count interval. Also, as $\Delta\phi = (2\pi/\lambda_0)\,\Delta R$,

$$f_D = \frac{1}{\lambda_0}\frac{\Delta R}{T_c} = \frac{v_R}{\lambda_0}, \text{Hz} \qquad (41)$$

for a one-way path, where v_R is the average radial component of velocity and f_D is the average Doppler frequency during the time T_c. For a two-way ranging system,

$$f_D = \frac{2v_R}{\lambda_0} \qquad (42)$$

It can be noted that if a value f_D is recorded during an interval T_c, a corresponding change in range ΔR has taken place during T_c. In this case, ΔR can represent either a true change in range or a change in excess range delay or a combination of the two. (Elsewhere ΔR has been used for total excess range due to water vapor or liquid water, but in this section ΔR is any arbitrary change or increment or range.) For an accuracy of 10^{-5} m/s in velocity T_c may be as low as 1 to 10 s when a spacecraft is near the Earth or another planet, or it may be as long as 1000 s when the spacecraft is in a cruise phase (Ref. 29).

B. Doppler Frequency Noise

Precise calculation of range delay due to the troposphere requires information concerning the water vapor, liquid water, and temperature profiles, but representative values can be calculated readily. Fewer data concerning Doppler frequency are available and it is somewhat more difficult to establish representative values for Doppler frequency noise. Both bulk changes in water vapor and liquid water content along the path and tropospheric scintillation involving scatter from turbulent irregularities can contribute to this noise. The term scintillation is usually applied to rather rapid variations of amplitude, phase, and angle of arrival. For considering tropospheric effects, it may be distintuished from refractive fading that results from the large-scale structure of the index of refraction and tends to involve amplitude variations of fairly large magnitude but of lower frequency than scintillation.

Because of the relations between phase, excess range delay, time delay, and Doppler frequency, the occurrence of phase scintillation implies also the occurrence of range and time delay jitter and Doppler noise. The noise is generated in proportion to the rate of change of phase as indicated by Eqs. (39) and (40). In some investigations of phase scintillation, records were taken showing the variation of phase with time. These allow the determination of corresponding Doppler frequency values. Using phase records obtained by Thompson, et al., (Ref. 30) in Hawaii, Armstrong, Woo, and Estabrook (Ref. 3) estimated the fractional Doppler frequency stability for propagation through the troposphere on Earth-space paths for a 1000-s count interval to be about 5×10^{-14} or less [σ_y (1000 s) $\sim 5 \times 10^{-14}$ where σ_y is referred to as an Allan variance]. It was estimated also that plasma scintillation at S-band, primarily involving the solar plasma contribution which dominates the ionospheric contribution, would cause noise corresponding to σ_y (1000 s) $\sim 3 \times 10^{-14}$. Minimum Doppler frequency noise due to the solar plasma is observed in the antisolar direction. Use of an X-band system is estimated to reduce the plasma noise to that corresponding to σ_y (1000 s) $\sim 3 \times 10^{-15}$. Thus it was inferred that tropospheric scintillation may dominate for the case of an X-band system. Also using data from Thompson, et al., (Ref. 30) and radiosonde data from Edwards Air Force Base, California, as well, Berman and Slobin (Ref. 18) have estimated a fractional Doppler frequency stability for two-way propagation and a 1000-s count interval as 1.6×10^{-14}.

C. Gravitational Waves

It is generally considered that gravitational waves may produce a fractional variation in Doppler frequency equal to or less than about 10^{-15} (Refs. 2 and 3). Thus detection of gravitational waves will require careful attention and efforts to minimize the effects of all sources of Doppler noise and instability. On sufficiently long paths, gravitational waves should impart a characteristic triple-impulse signature to the Doppler record. The three impulses arise from buffeting of the spacecraft and Earth by the passing gravitational wave and involve the travel times between the Earth and spacecraft. For example, the gravitational wave might first buffet the Earth and the antenna of the telecommunication system and thus produce an immediate corresponding Doppler impulse in the received signal. Then the gravitational wave might buffet the spacecraft, and this would produce an impulse in the Doppler record after a time delay corresponding to the travel time from the spacecraft to Earth. Finally, a third impulse would appear in the Doppler record of the received signal, corresponding to the original buffeting of the Earth antenna, but delayed by the travel time from the Earth to the spacecraft and back. The form of the actual sequence of impulses would depend upon the geometrical configuration of the Earth and spacecraft and the direction of travel of the gravitational wave. An effect due to clock speedup is also expected (Ref. 2). As the periods of gravitational impulses are long (10 to 10,000 s), long telecommunications paths involving round-trip travel times of about 1000 s and longer are required for the detection of gravitational waves by the technique under discussion.

V. Excess Range Delay in Terms of Total Water Vapor and Liquid Water Content

A. Delay Due to Liquid Water

Consideration is given in this section to expressing excess range delay in terms of the total masses of water vapor and liquid water in a vertical column. Expressions of this type have been in use (Ref. 15), and the basis for them will now be examined. The case of the small water droplets of a cloud is the simplest to analyze. For this purpose, Eq. (33) is repeated below.

$$m - 1 = \frac{\chi}{2} = \frac{3NV}{2}\left(\frac{n^2-1}{n^2+2}\right) \qquad (33)$$

Range delay ΔR_2 for a zenith path through a uniform cloud of thickness h is given by

$$\Delta R_2 = (m-1)\,h \qquad (43)$$

which is merely a statement of Eq. (34) for a uniform cloud. The total liquid water content in a vertical column M_L is given for the uniform case by

$$M_L = NVh\rho \qquad (44)$$

where N is the number of droplets per unit volume, V is the volume of an individual droplet, h is the vertical extent of the cloud, and ρ is the density of water, namely 1000 kg/m^3 in SI units. Of the four factors of Eq. (44), all but ρ already appear in the expression for ΔR_2. The remaining quantities in the expression for ΔR_2 are $3/2\ (n^2 - 1)/(n^2 + 2)$, which equals $(3/2)(0.967) = 1.45$ for $f = 3$ GHz. If $\rho = 10^3$ is to be introduced into Eq. (35) where it did not originally appear, so that ΔR_2 can be expressed in terms of M_L, a factor of 10^{-3} must be introduced to compensate. Thus

$$\Delta R_2 = 1.45 \times 10^{-3} M_L, \text{ m} \qquad (45)$$

with M_L for the example of Section III having the value of $(10^{-6})(10^3)(10^3) = 1$ kg/m^2, where the three factors represent NV, h, and ρ respectively. If it is desired to express ΔR_2 in cm and M_L in g/cm^2, then

$$\Delta R_2 = 1.45\, M_L, \text{ cm} \qquad (46)$$

with $M_L = 0.1$ g/cm^2 for the same example of Section III. For other frequencies, the value of $(n^2-1)/(n^2+2)$ will change only very slightly, so Eqs. (45) and (46) are generally applicable with reasonable accuracy. The expressions apply to the small droplets of clouds, or, in general, when Rayleigh scattering can be assumed to take place. The droplets of clouds actually vary in size such that one should use a summation $\Sigma N_i V_i$ in place of NV, but the simple form of Eq. (33) is sufficient for present purposes.

B. Delay Due to Water Vapor

Consider next the case of water vapor. The applicable expression in this case is

$$\Delta R_w = 3.323 \times 10^{-7} \int \rho\, dl + 1.731 \times 10^{-3} \int \frac{\rho}{T}\, dl \qquad (13)$$

with ρ in g/m^3 or

$$\Delta R_w = 3.323 \times 10^{-4} \int \rho\, dl + 1.731 \int \frac{\rho}{T}\, dl \qquad (47)$$

with ρ in kg/m^3. The delay is a function of temperature as well as total water vapor content. If T is taken to be 281.65 K (the temperature in a standard atmosphere at an elevation above sea level of 1 km) as was assumed in Section II,

$$\Delta R_1 = 6.48 \times 10^{-3} M_V, \text{ m} \qquad (48)$$

where M_V, the mass of water vapor in a vertical column, equals $\int \rho\, dl$, and, in the example of Section II with $\rho =$

$7.5\ g/m^3 = 7.5 \times 10^{-3}\ kg/m^3$ at the surface and a scale height of 2 km, is 15 kg/m^2. If it is desired to express ΔR_1 in cm and M_V in g/cm^2, then

$$\Delta R_i = 6.48\, M_V, \text{cm} \qquad (49)$$

For the same example of Section II, $M_V = 1.5\ g/cm^2$ and $\Delta R_1 = 9.72$ cm. Equations (48) and (49) apply strictly only for a constant or average value of temperature of 281.65 K, and choice of this value, while reasonable, was arbitrary. However, the equations can be used for rough estimates of ΔR_1 if deisred, and if the temperature profile does not depart excessively from the constant value assumed here.

C. Combined Delay

The combined delay due to water vapor and small water droplets on a zenith path is given roughly by

$$\Delta R = \Delta R_1 + \Delta R_2 = 6.48\ M_V + 1.45\, M_L, \text{cm} \qquad (50)$$

with M_V and M_L in g/cm^2. The delay due to water vapor ΔR_1 is actually a function of temperature as well as the mass of water vapor in a vertical column M_L. If information on temperature and water vapor profiles are available, Eq. (13) should be used for ΔR_1 instead of Eqs. (48 through 50) to obtain a better estimate.

VI. Conclusion

The excess range delay due to water vapor and liquid water content of the troposphere require attention when high precision is required for range measurement on Earth-space paths. The physical factors affecting excess range delay have been discussed and illustrative calculations of range delay have been presented in this report. The use of radiometer techniques for continuous monitoring of the range delay and Doppler frequency due to water vapor appears to be advantageous when high precision is required. The various possible systems for accomplishing this purpose should be carefully considered. The same general principles have been used for remotely sensing the water vapor and liquid water content of the atmosphere from Nimbus satellites (Refs. 31 and 32), but in these applications total water vapor content, $\int \rho\, dh$, and not $\int (\rho/T)\, dh$, is obtained.

Excess range delay at an elevation angle θ, $\Delta R(\theta)$, may generally be related to delay for a zenith path (θ = 90 deg) for elevation angles greater than about 10 deg by

$$\Delta R(\theta) = \frac{\Delta R(\theta = 90\ \text{deg})}{\sin\theta} \qquad (23)$$

For clouds, information on the thickness and liquid water density of a cloud is required to estimate range. For estimating excess range delay through rain as accurately as possible, one needs to take into account that average rain rates tend to be less than point rain rates for heavy rains (Refs. 25 and 26).

The separate but related topic of Doppler frequency noise has been considered briefly. Whereas range delay involves the integral of the index of refraction minus unity along a path, Doppler frequency noise involves the time rate of change of the integral. Range delay can be analyzed as involving propagation in a locally homogeneous medium, but consideration of Doppler noise requires attention to scintillation, involving scatter from inhomogeneities as well. Variations in range delay imply Doppler frequency noise, and Doppler frequency noise implies jitter in range. Correction for range delay allows increased precision in range measurement. Minimizing Doppler frequency noise of interplanetary origin by moving to higher frequencies increases the probability of detecting weak effects such as gravitational waves, but Doppler noise of tropospheric origin may then dominate.

When striving for the highest possible precision in range measurement, the limitations posed by the state of knowledge of the velocity of light should be kept in mind. The value of c of 299,792,458 m/s involves a fractional uncertainty $\Delta c/c$ of $\pm 4 \times 10^{-9}$ (Ref. 33). Specifying c to nine significant figures may seem impressive, but the fractional uncertainty in c corresponds to an uncertainty in velocity of 1.2 m/s and an uncertainty in meters in one-way range of 1.2 times the propagation times in seconds. For spacecraft near Saturn, say at 10 AU, the corresponding uncertainty in absolute range is about 6 km. This consideration should not be regarded as unduly discouraging. When using the VLBI technique, for example, it is the difference in range to the spacecraft from two locations that is important and not the absolute range. In other situations, it is the consistency and precision of range measurements that is essential, rather than accuracy of absolute range. One should take care, however, not to imply that the precisions of a few meters or centimeters in range measurement on long paths represent the accuracies to which absolute range can be measured.

Acknowledgments

I would like to express my appreciation to T. A. Komarek, E. K. Smith, J. G. Meeker, S. D. Slobin, and B. Gary for helpful discussions and for encouraging and supporting the effort on this report.

References

1. Anderson, J. D., and Estabrook, F. B., "Application of DSN Spacecraft Tracking Technology to Experimental Gravitation," *J. of Spacecraft and Rockets*, Vol. 16, pp. 120-125, March-April 1979.
2. Berman, A. L., "The Gravitational Wave Detection Experiment: Description and Anticipated Requirements," in *The Deep Space Network Progress Report 42-46*, Jet Propulsion Laboratory, Pasadena, Calif., pp. 100-108, May and June 1978.
3. Armstrong, J. W., Woo, R., and Estabrook, F. B., "Interplanetary Phase Scintillation and the Search for Very Low Frequency Gravitational Radiation," *Astrophysical Journal*, Vol. 230, pp. 570-749, June 1, 1979.
4. Smith, E. K., and Weintraub, S., "The Constants in the Equation for Atmospheric Refractive Index at Radio Frequencies," *Proc. IRE*, Vol. 41, pp. 1035-1037, August 1953.
5. List, R. J., *Smithsonian Meteorological Tables*, Sixth Revised Edition, Washington, D.C., Smithsonian Institution, 1958.
6. Crane, R. K., "Refraction Effects in the Neutral Atmosphere," in *Methods of Experimental Physics*, Vol. 12, *Astrophysics*, Part B: *Radio Telescopes* (M. L. Meeks, ed.), pp. 186-200. New York: Academic Press, 1976.
7. Hopfield, H. S., "Tropospheric Effect on Electromagnetically Measured Range: Prediction from Surface Weather Data," *Radio Science*, Vol. 6, pp. 357-367, March 1971.
8. Waters, J. W., "Absorption and Emission by Atmospheric Gases," in *Methods of Experimental Physics*, Vol. 12, *Astrophysics*, Part B: *Radio Telescopes* (M. L. Meeks, ed.), pp. 142-176. New York: Academic Press, 1976.
9. Guiraud, F. E., Howard, J., and Hogg, D. C., "A Dual-channel Microwave Radiometer for Measurement of Precipitable Water Vapor and Liquid," *IEEE Trans. on Geoscience Electronics*, Vol. GE-17, pp. 129-136, October 1979.
10. Hogg, D. C., "Ground-based Remote Sensing and Profiling of the Lower Atmosphere using Radio Wavelengths," *IEEE Trans. on Antennas and Propagation*, Vol AP-28, pp. 281-283, March 1980.
11. Wu, S. C., "Frequency Selection and Calibration of a Water Vapor Radiometer," in *The Deep Space Network Progress Report 42-43*, Jet Propulsion Laboratory, Pasadena, Calif., pp. 67-81, Nov. and Dec. 1977.
12. Winn, F. B., et al., "Atmospheric Water Vapor Calibrations: Radiometer Technique," in *The Deep Space Network Progress Report 42-32*, Jet Propulsion Laboratory, Pasadena, Calif., pp. 38-44, Jan and Feb. 1976.

13. Claflin, E. S., Wu, S. C., and Resch, G. M., "Microwave Radiometer Measurement of Water Vapor Path Delay: Data Reduction Techniques," in *The Deep Space Network Progress Report 42-48*, Jet Propulsion Laboratory, Pasadena, Calif., pp. 22-30, Sept. and Oct. 1978.

14. Batelaan, P. D., and Slobin, S. D., "DSN Water Vapor Radiometer Development – Recent Work, 1978," in *The Deep Space Network Progress Report 42-48*, Jet Propulsion Laboratory, Pasadena, Calif., pp. 129-135, Sept. and Oct. 1978.

15. Slobin, S. D., and Batelaan, P. D., "DSN Water Vapor Radiometer – Tropospheric Range Delay Calibration," in *The Deep Space Network Progress Report 42-49*, Jet Propulsion Laboratory, Pasadena, Calif., pp. 136-145, Nov. and Dec. 1978.

16. CCIR, "Attenuation by Atmospheric Gases," Report 719, pp. 97-102, in *Recommendations and Reports of the CCIR, 1978*, Vol. V, *Propagation in Non-ionized Media*, Geneva: ITU, 1978.

17. *U.S. Standard Atmosphere, 1976*, sponsored by NOAA, NASA, USAF. Washington, D.C.: Supt. of Documents, U.S. Government Printing Office, 1976.

18. Berman, A. L., and Slobin, S. D., "Tropospheric Path Length Fluctuation in Temperate Semiarid Locales: Application to the Gravitational Wave Detection Experiment," in *The Deep Space Network Progress Report 42-55*, Jet Propulsion Laboratory, Pasadena, Calif., pp. 79-85, Nov. and Dec. 1979.

19. Ramo, S., Whinnery, J. R. and Van Duzer, T., *Fields and Waves in Communication Electronics*, New York: Wiley, 1965.

20. Zufferey, C. H., *A Study of Rain Effects on Electromagnetic Waves in the 1-600 GHz Range*, M. S. Thesis, Boulder, Co.: Department of Electrical Engineering, U. of Colorado, 1972 (reprinted in 1979).

21. Hogg, D. C., and Chu, T. S., "The Role of Rain in Satellite Communications," *Proc. IEEE*, Vol. 63, pp. 1308-1331, Sept. 1975.

22. Gunn, K. L. S., and East, T. W. R., "The Microwave Properties of Precipitation Particles," *Quart. J. Roy, Meteor. Soc.*, Vol. 80, pp. 522-545, 1954.

23. Valley, S. L. (ed.), *Handbook of Geophysics and Space Environment*, Air Force Cambridge Research Laboratories, New York: McGraw-Hill, 1965.

24. Setzer, D. E., "Computed Transmission through Rain at Microwave and Visible Frequencies," *Bell System Tech. Jour.*, Vol. 49, pp. 1873-1892, Oct. 1970.

25. Karl, R., Wallace, R., and Kinal, G., *A Propagation Effects Handbook for Satellite System Design, A Summary of Propagation Impairments on 10-100 GHz Satellite Links with Techniques for System Design*, Washington, D.C.: NASA Communications Division, NASA Headquarters, March 1980.

26. Crane, R. K., "Prediction of Attenuation by Rain," *IEEE Trans. on Communications*, Vol. COM-28, pp. 1717-1733, Sept. 1980.

27. van de Hulst, H. C., *Light Scattering by Small Particles*. New York: Wiley, 1957.

28. Kerker, M., *The Scattering of Light and Other Electromagnetic Radiation*, New York: Academic Press, 1969.

29. Moyer, T. D., *Mathematical Formulation of the Double-Precision Orbit Determination Program (DPODP)*, Technical Report 32-1527, Jet Propulsion Laboratory, Pasadena, Calif., May 15, 1971.

30. Thompson, M. C., Wood, L. E., Janes, H. B., and Smith, D., "Phase and Amplitude Scintillations in the 10 to 40 GHz band," *IEEE Trans. on Antennas and Propagation*, Vol. AP-23, pp. 792-797, Nov. 1975.

31. Grody, N. C., "Remote Sensing of Atmospheric Water Content from Satellites using Microwave Radiometry," *IEEE Trans. on Antennas and Propagation*, Vol. AP-24, pp. 155-162, March 1976.

32. Chang, A. T. C., and Wilheit, T. T., "Remote Sensing of Atmospheric Water Vapor, Liquid Water, and Wind Speed at the Ocean Surface by Passive Microwave Techniques from the Nimbus 5 Satellite," *Radio Science*, Vol. 14, pp. 793-802, Sept.-Oct. 1979.

33. Evenson, K. M., "The Development of Direct Optical Frequency Measurement and the Speed of Light," *ISA Transactions*, Vol. 14, pp. 209-216, 1975.

Table 1 Saturation water vapor pressure, e_s in mb [adapted from Smithsonian Meteorological Tables, 1958 (Ref. 5)]

T, °C	e_s, mb	T, °C	e_s, mb
-30	0.5	20	23.4
-20	1.3	22	26.4
-10	2.9	24	29.8
0	6.1	26	33.6
2	7.1	28	37.8
4	8.1	30	42.4
6	9.3	32	47.6
8	10.7	34	53.2
10	12.3	36	59.4
12	14.0	38	66.3
14	16.0	40	73.8
18	20.6		

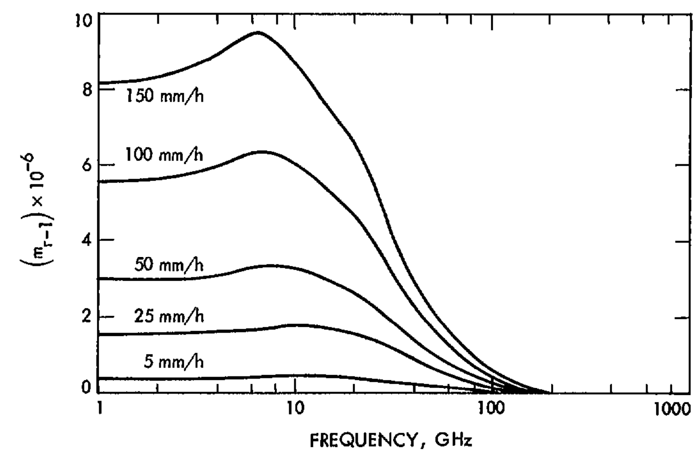

Fig. 1. The real part of the equivalent index of refraction minus unity (m_r - 1) of a medium consisting of raindrops in empty space, as a function of frequency (Ref. 20) (Temperature 20°C; Laws and Parsons distribution)

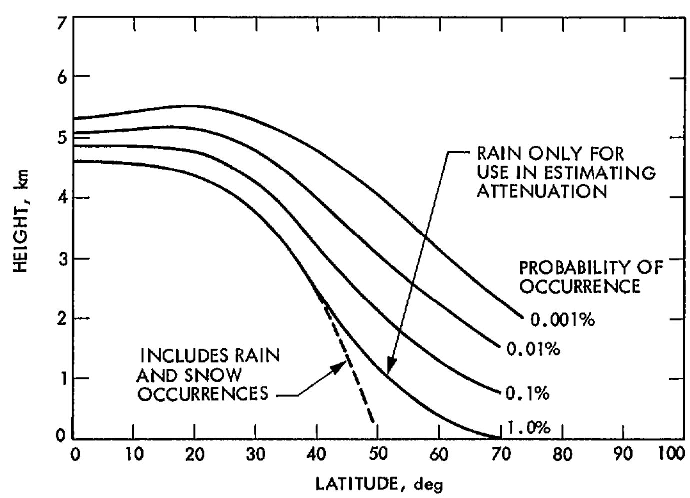

Fig. 2. Height of the 0°C isotherm as a function of latitude and probability of occurrence (Ref. 26)

Appendix

Relation Between Water Vapor Pressure and Density

The perfect gas law in the form applying to one molecular weight of gas is

$$pv = RT \qquad \text{(A-1)}$$

where, in SI units, p is pressure in $\mathrm{N/m^2}$; v is specific volume in $\mathrm{m^3}$; R is the gas constant, 8.314×10^3 J/(K kg mol), where J stands for joules and T is temperature in kelvins. To obtain density ρ in $\mathrm{kg/m^3}$, use

$$\rho = \frac{M}{v} = \frac{pM}{RT} \qquad \text{(A-2)}$$

where M is molecular weight in kg mol. Also note that

$$\frac{p}{T} = \frac{R}{v} = \frac{R\rho}{M} \qquad \text{(A-3)}$$

If we apply Eq. (A-2) to water vapor and thus set p equal to e, the water vapor pressure in $\mathrm{N/m^2}$, and M equal to 18.02 kg,

$$\rho = \frac{e\ 18.02}{8.3143 \times 10^3 T} = \frac{2.167 \times 10^{-3}\, e}{T}, \mathrm{kg/m^3} \qquad \text{(A-4)}$$

If e is to be expressed in mb, however, rather than $\mathrm{N/m^2}$,

$$\rho = \frac{0.2167e}{T}, \mathrm{kg/m^3} \qquad \text{(A-5)}$$

Finally for $\rho = \mathrm{g/m^3}$ and e in mb,

$$\rho = \frac{216.7\, e}{T}, \mathrm{g/m^3} \qquad \text{(A-6)}$$